ACS Sustainable Chemistry & Engineering

pubs.acs.org/journal/ascecg

Letter

Improved Mass Transport of 5-Hydroxymethylfurfural Electrochemical Reduction through Gas−Liquid Cocirculation

Mohammad Peirow Asfia, Walter A. Parada, Lukas Klerner, Angelina Cuomo, Urban Sajevic, Karl J. J. Mayrhofer, and Pavlo Nikolaienko*

Cite This: ACS Sustainable Chem. Eng. 2025, 13, 12323−12327

Read Online

ACCESS | Metrics & More | Article Recommendations | Supporting Information

ABSTRACT: Mass transfer phenomena significantly influence the conversion rate and product distribution in the 5-hydroxymethylfurfural (HMF) electrochemical reduction to value-added products. This study proposes a cost-effective approach to enhance the production rate and selectivity toward 2,5-bis(hydroxymethyl)furan (BHMF) as the target product. Cocirculating the electrolyte with an inert gas across the electrode surface increases the conversion rate and selectivity toward alcohol formation by 50% and 75%, respectively. This improvement is attributed to enhanced reactant adsorption and product desorption, along with improved mobility of forming H_2 microbubbles away from the surface, which increases the availability of active sites for the hydrogenation reaction. Simulations of the hydrodynamic behavior of the electrolyte near the working electrode during gas purging suggest improved convection near the electrode.

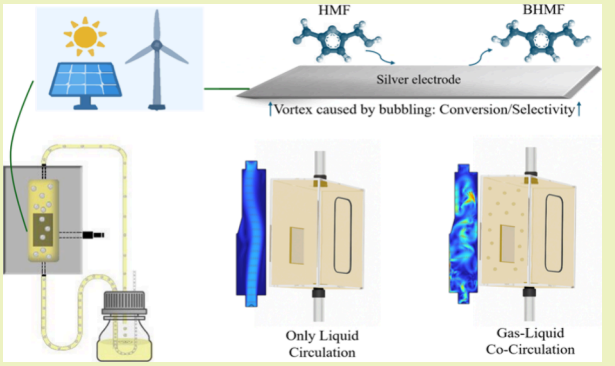

KEYWORDS: *5-Hydroxymethylfurfural, Mass transfer, Gas−liquid cocirculation, High-value derivatives, Electrochemical reduction*

INTRODUCTION

In the realm of chemical industries, the electrochemical conversion of biomass-derived molecules into value-added products is crucial for sustainable and environmentally friendly processes.[1,2] One such molecule is 5-hydroxymethylfurfural (HMF),[3,4] a versatile reactant for a wide range of compounds with applications in polymers and biofuels.[5,6] Researchers have extensively investigated the electrochemical reduction of HMF into valorized chemicals and precursors, including 2,5-bis(hydroxymethyl)furan (BHMF)[7] and 5,5′-bis(hydroxymethyl)hydrofuroin (BHH).[8]

Despite this progress, mass transport limitations remain a significant obstacle in achieving efficient HMF conversion, affecting reaction rates and product distribution.[9] Various strategies, such as biphasic solvent systems[10] and designing electrodes to improve mass transfer,[11] have been proposed to overcome these limitations. Sanghez de Luna et al.[12] demonstrated that using 3D expanded foam electrodes enhances the catalyst's active surface area, reducing mass transfer constraints and boosting both conversion rates and BHMF yields in HMF electrochemical reduction (HMF-ER). Recent studies in biphasic electrocatalysis have shown how phase separation, solvent polarity, and viscosity can strongly affect mass transport and product selectivity in electrochemical biomass conversion.[13,14]

Several researchers have explored innovative electrochemical cell designs to overcome mass transfer limitations in HMF electrochemical conversion.[15−17] In one such study, Delparish et al.[18] investigated how reactor design and cell configuration influence HMF electrochemical oxidation and found that adsorption of HMF and its intermediates drives the mechanism. Their results showed that an undivided microreactor enhances adsorption, but such specialized reactor designs often prove costly and require significant design complexity.

Here, we propose a practical approach to mitigate mass transport limitations, exemplified by HMF-ER. Alongside forced electrolyte convection (continuous flow),[19,20] purging gas near the electrode surface can increase local electrolyte flow while removing electrochemical products and gas bubbles, synergistically enhancing mass transfer dynamics. In typical electrochemical setups, N_2 is already and inevitably introduced to remove dissolved O_2, as its reduction reaction (ORR) could lead to the formation of H_2O_2 and is detrimental for overall FE, which competes with HMF reduction. Instead of bubbling N_2 into the reservoir (purging and blanketing), we redirected this flow directly into the electrolyte inlet, enabling it to

Received: May 8, 2025
Revised: July 25, 2025
Accepted: July 25, 2025
Published: July 30, 2025

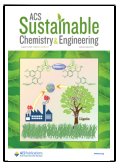

simultaneously serve its original purpose and drive interfacial convection.[21] We validate the effectiveness of this cocirculation strategy using experimental electrochemical techniques and computational simulations.

RESULTS AND DISCUSSION

We utilized a planar electrode for electrochemical measurements to evaluate the applicability of the bubbling-enhanced convection approach. Such electrodes' defined active surface area leads to mass transfer limitations for both reactants and products.[22] We employed silver foil as the catalyst for the HMF electrochemical reduction because of the possibility of forming different products, namely, BHMF (the primary product), BHH (the dimer), polymerization to humins (others),[23] and hydrogen evolution reaction (HER), all of which strongly depend on a mass transfer phenomenon.[24] This broad range of formable products allows us to thoroughly assess how our cocirculation approach affects product distribution in HMF-ER.

An in-house designed two-compartment electrolysis cell was used for all electrochemical experiments (Scheme 1),[25] with detailed specifications in the Supporting Information. The headspace gases were immediately directed into a gas chromatograph (GC) for analysis, while the liquid products were quantified using high-performance liquid chromatography (HPLC).

Scheme 1. Schematic Representation of the Electrochemical Divided H-Type Cell

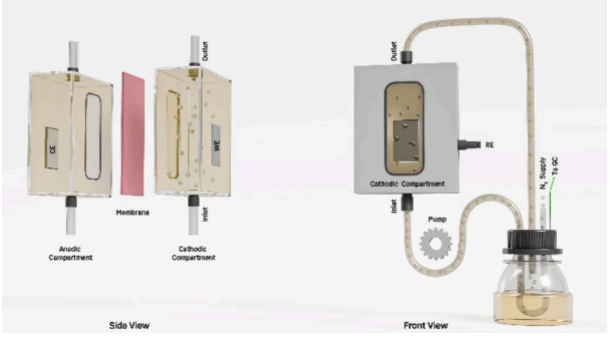

All electrochemical measurements were performed in a sodium carbonate electrolyte (pH 9.2) containing 20 mM HMF, which was optimal for minimizing extensive HMF chemical degradation.

Circulating only the electrolyte (blanketing the electrolyte with N_2 to remove dissolved air from the system) at a flow rate of up to 5 mL min^{-1} led to a significantly low HMF conversion rate of only 30% at an applied potential of −0.65 V vs E_{RHE} over 2 h chronoamperometry. Figure 1 shows that BHMF accounts for only 40% selectivity, while 12.5% is attributed to BHH. The remaining fraction consists primarily of undesirable polymerization products. Purging 1 mL min^{-1} N_2 increases the HMF conversion rate to 40%, and the BHMF selectivity rises to nearly 70%, a net 75% increase compared to the condition without gas purging. The reduced selectivity toward BHH and other undesired products may result from enhanced mass transfer. Table 1 (complete data available in SI Table S1) shows that the N_2 gas purge at 1 mL min^{-1} into the reaction compartment instead of a blanket feed over the electrolyte reservoir reduces the Faradaic efficiency (FE) for HER from

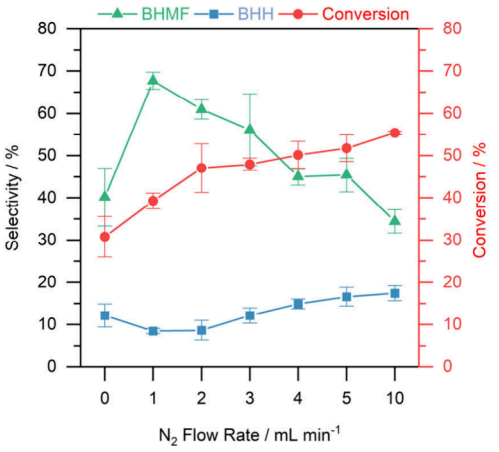

Figure 1. HMF conversion (second y axis) and main product selectivity of electrochemical reduction of HMF, influenced by the flow of N_2 in the system (20 mM HMF, 0.1 M sodium carbonate buffer, 2 h chronoamperometry at an applied potential of −0.65 V vs E_{RHE}, error bars obtained from at least three repetitions).

Table 1. Total Charge Passed (TCP) and Faradaic Efficiency of the Products Influenced by the Flow Rate of N_2 in the System[a]

Flow rate /mL min^{-1}	TCP/ C cm^{-2}	FE BHMF/%	FE BHH/%	FE H_2/%
0	8.6	38.2	7.1	22.9
1	10.5	72.6	4.6	9.2
2	11.3	73.4	5.1	15.2
3	11.2	62.1	7.1	22.7
4	11.6	56.9	8.6	23.4
5	11.8	58.3	10.7	20.8
10	12.4	43.9	11.1	21.8

[a]20 mM HMF, 0.1 M sodium carbonate buffer, 2 h chronoamperometry at applied potential of − 0.65 V vs E_{RHE}.

22.9% to 9.2%. These results indicate that mass transfer limitations not only hinder the HMF conversion rate but also reduce the selectivity toward valuable products.

Without gas cocirculation of the system, both reactant adsorption and product desorption appear to be mass-transfer-limited, leading to low HMF conversion (30%). Hence, restricted HMF availability at the electrode surface favors the Tafel/Heyrovsky pathway to H_2 formation over the reaction with HMF ketyl radical intermediates to form BHMF (Scheme 2). Consequently, these intermediates are more likely to

Scheme 2. Mechanism Pathway of HMF Electrochemical Reduction Towards BHMF and BHH on Silver[a]

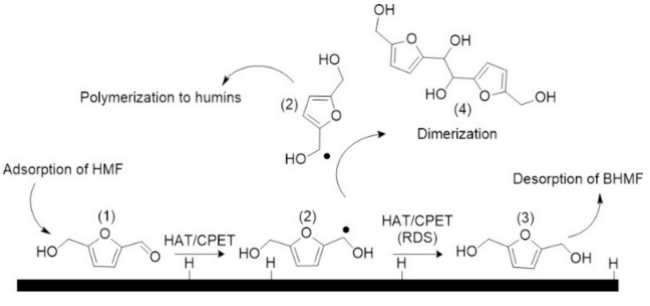

[a](1) HMF, (2) HMF ketyl radical, (3) BHMF, and (4) BHH.

https://doi.org/10.1021/acssuschemeng.5c04334
ACS Sustainable Chem. Eng. 2025, 13, 12323−12327

dimerize and form BHH or polymerize. Additionally, a higher HER (~22%) leads to electrode surface coverage by H_2 microbubbles, further limiting the availability of active sites. Introducing an inert gas like nitrogen into the electrolyte flow enhances convection near the electrode surface, which facilitates adsorption and desorption processes within the electrochemical double layer (EDL). Therefore, interactions between ketyl radicals and adsorbed hydrogen atoms are more probable, which increases the level of BHMF formation and reduces the level of HER. Furthermore, N_2 bubbles displace small H_2 bubbles away from the surface, providing more active sites for hydrogenation reactions. These two factors contribute to the observed improvements in mass transfer when cocirculating gas.

Despite the improved mass transfer and increased HMF conversion at higher gas flow rates, BHMF selectivity drops by 10% once the flow rate exceeds a critical threshold of 1 mL min^{-1}. Figure 1 shows that a flow rate of 2 mL min^{-1} lowers BHMF selectivity by 10% compared to 1 mL min^{-1}, while a further increase to 10 mL min^{-1} reduces selectivity to 34%, even lower than those in experiments without gas purging. In contrast, the selectivity and FE for BHH and HER increase with increasing N_2 flow rates. Scheme 2 shows the HMF-ER on silver, which rationalizes the observed phenomenon.

Based on this mechanism, HMF undergoes hydrogenation via proton-coupled electron transfer (PCET) or hydrogen atom transfer (HAT), forming a ketyl radical intermediate.[26] This intermediate either proceeds through another hydrogenation step to form BHMF or dimerizes/polymerizes. The second hydrogenation step is the rate-determining step (RDS),[27] requiring sufficient reaction time and conditions. At higher nitrogen flow rates, the probability of completing this step decreases, so ketyl radical intermediates and adsorbed hydrogen accumulate, which fosters dimerization, polymerization, and HER.

Table 1 shows that introducing 1 mL min^{-1} N_2 flow lowers the HER Faradaic efficiency, but higher flow rates reverse this trend. At the same time, BHMF selectivity drops, while BHH and polymer formation increase. This shift reflects a change in reaction dynamics: faster electrolyte flow and bubble-induced vortices increase the local turbulence near the electrode, accelerating ketyl radical removal from the interface. As a result, the radicals lose the chance to undergo the second hydrogenation step and instead follow alternative pathways like dimerization and polymerization, which are less surface-dependent on silver.[12,22,28,29] At higher flow, more surface sites become available for H adsorption, and the adsorbed hydrogen atoms recombine to form H_2, which increases the HER activity.

We use COMSOL simulations to support this interpretation and highlight the effect of N_2 bubbling as a cocirculation mechanism. COMSOL simulations demonstrate that nitrogen bubbling significantly increases convection near the electrode, which improves the HMF mass transport and boosts conversion in the electrochemical reduction reaction. Figure 2 illustrates a significant growth of the flow velocity with rising gas feed rates. Notably, the increase in convection from 0 mL min^{-1} to 1 mL min^{-1} is comparable to that from 1 mL min^{-1} and 10 mL min^{-1}, indicating that higher bubbling rates offer only marginal gains (Figures S4–S11 and Table S2 provide further details).

As a proof of concept, we also performed electrochemical measurements on planar glassy carbon (also on copper

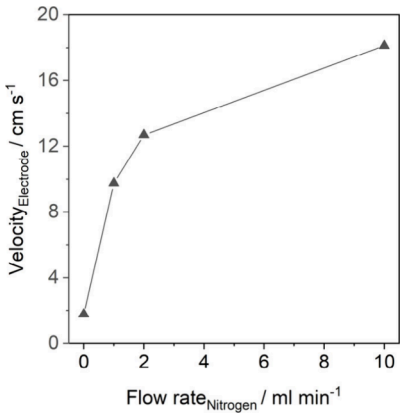

Figure 2. Simulated electrolyte velocity on the electrode surface when bubbling N_2 through the electrochemical cell. The values displayed were obtained by averaging parameters at a steady state (0.5–4 s in Figure S2).

electrode, Figure S12), a recognized catalyst for HMF dimerization.[25] Figure 3 shows that, although glassy carbon is a nonmetallic electrode with minimal adsorption and desorption of reactive species, the cocirculation approach raises HMF conversion from 20% to 47% by increasing local fluid velocity and alleviating mass transfer limitations. This strategy also affects the product selectivity of HMF on glassy carbon.

As shown in Figure 3a, the introduction of N_2 reduces BHH selectivity. The proposed mechanism for BHH formation on glassy carbon involves inner- and outer-sphere reactions,[23] each yielding distinct stereoisomers. The outer-sphere pathway produces the *meso* isomer and polymerization products, whereas the inner-sphere predominantly yields racemic (*DL*) BHH (Table S3 provides detailed information, including FE, formation rate, and *meso* and *DL* formation). Without gas flow, ketyl radicals stay near the surface and couple with each other to form *DL*-BHH (Figure 3b). Introducing N_2 gas flow

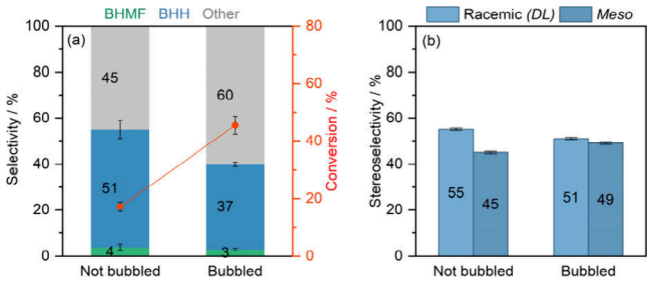

Figure 3. a) Main product selectivity (bars) and conversion of HMF (red line) and b) stereoselectivity of BHH in the electrochemical reduction of HMF on glassy carbon, with and without the flow of N_2 in the system (20 mM HMF, 0.1 M sodium carbonate buffer, 2 h chronoamperometry at an applied potential of −0.8 V vs E_{RHE}, error bars obtained from at least three repetitions).

detaches these radicals from weak $\pi-\pi$ interaction with the glassy carbon surface,[23] which promotes uncontrolled polymerization. These results confirm that gas–liquid cocirculation is not a catalyst-specific approach.

CONCLUSION

We introduced a simple yet effective cocirculation strategy in which purging an inert gas such as N_2 directly into the

https://doi.org/10.1021/acssuschemeng.5c04334
ACS Sustainable Chem. Eng. 2025, 13, 12323−12327

electrolyte inlet significantly improves the electrochemical reduction of HMF by alleviating mass transport limitations. This design enhances HMF conversion and modulates product distribution by accelerating the delivery of reactants to the electrode surface and the removal of products and bubbles from it, thereby improving reaction efficiency.

COMSOL simulations confirm that cocirculation increases local flow velocity near the electrode surface. At moderate N_2 flow rates (up to 1−2 mL min^{-1}), BHMF selectivity improves due to enhanced interaction between ketyl intermediates and adsorbed hydrogen, along with more accessible active sites from efficient H_2 bubble displacement.

However, further increasing the gas flow rate above 1 mL min^{-1} leads to a decline in BHMF selectivity. We attribute this to the reduced residence time of ketyl radicals near the surface, which prevents the completion of the second hydrogenation step. These radicals are instead diverted toward dimerization or polymerization, leading to increased BHH and humin formation.

■ ASSOCIATED CONTENT

Supporting Information

The Supporting Information is available free of charge at https://pubs.acs.org/doi/10.1021/acssuschemeng.5c04334.

Specification of materials and chemicals, electrode preparation, and flow-cell assembly. Description of electrochemical measurements, operating conditions, and evaluation methods. Details of the COMSOL simulation setup and parameters. Supplementary figures showing cocirculation setup, bubble flow visualization, and additional product analysis. Includes video documentation of bubble behavior, tables of electrochemical data, and reference values used in the main text (PDF)

Video file for Figure S2b (MP4)

Video S1a (MP4)

Video S1b (MP4)

Video S1c (MP4)

■ AUTHOR INFORMATION

Corresponding Author

Pavlo Nikolaienko − *Forschungszentrum Jülich GmbH, Helmholtz Institute Erlangen-Nürnberg for Renewable Energy (IET-2), 91058 Erlangen, Germany;* orcid.org/0000-0002-1508-7589; Email: p.nikolaienko@fz-juelich.de

Authors

Mohammad Peirow Asfia − *Forschungszentrum Jülich GmbH, Helmholtz Institute Erlangen-Nürnberg for Renewable Energy (IET-2), 91058 Erlangen, Germany; Department of Chemical and Biological Engineering, Friedrich-Alexander University Erlangen-Nürnberg, 91058 Erlangen, Germany;* orcid.org/0000-0002-6653-5919

Walter A. Parada − *Forschungszentrum Jülich GmbH, Helmholtz Institute Erlangen-Nürnberg for Renewable Energy (IET-2), 91058 Erlangen, Germany; Department of Chemical and Biological Engineering, Friedrich-Alexander University Erlangen-Nürnberg, 91058 Erlangen, Germany;* orcid.org/0000-0002-5413-1917

Lukas Klerner − *Forschungszentrum Jülich GmbH, Helmholtz Institute Erlangen-Nürnberg for Renewable Energy (IET-2), 91058 Erlangen, Germany; Department of Chemical and Biological Engineering, Friedrich-Alexander University Erlangen-Nürnberg, 91058 Erlangen, Germany*

Angelina Cuomo − *Forschungszentrum Jülich GmbH, Helmholtz Institute Erlangen-Nürnberg for Renewable Energy (IET-2), 91058 Erlangen, Germany; Department of Chemical and Biological Engineering, Friedrich-Alexander University Erlangen-Nürnberg, 91058 Erlangen, Germany*

Urban Sajevic − *Forschungszentrum Jülich GmbH, Helmholtz Institute Erlangen-Nürnberg for Renewable Energy (IET-2), 91058 Erlangen, Germany; Department of Chemical and Biological Engineering, Friedrich-Alexander University Erlangen-Nürnberg, 91058 Erlangen, Germany;* orcid.org/0009-0009-8038-043X

Karl J. J. Mayrhofer − *Forschungszentrum Jülich GmbH, Helmholtz Institute Erlangen-Nürnberg for Renewable Energy (IET-2), 91058 Erlangen, Germany; Department of Chemical and Biological Engineering, Friedrich-Alexander University Erlangen-Nürnberg, 91058 Erlangen, Germany;* orcid.org/0000-0002-4248-0431

Complete contact information is available at: https://pubs.acs.org/10.1021/acssuschemeng.5c04334

Author Contributions

Mohammad Peirow Asfia, Pavlo Nikolaienko, and Karl J. J. Mayrhofer contributed to the manuscript's writing and the topic's conceptualization. Mohammad Peirow Asfia performed the electrochemical measurements and the analytical quantification. Walter A. Parada performed the computational simulations. Lukas Klerner, Angelina Cuomo, and Urban Sajevic contributed to reviewing and refining the manuscript.

Notes

The authors declare no competing financial interest.

■ ACKNOWLEDGMENTS

This research has been funded by the Deutsche Forschungsgemeinschaft (DFG, German Research Foundation) under Germany's Excellence Strategy − Exzellenzcluster2186 "The Fuel Science Center" − ID: 390919832.

■ REFERENCES

(1) Zhang, W.; Wang, Z.; Huang, J.; Jiang, Y. Zirconia-Based Solid Acid Catalysts for Biomass Conversion. *Energy Fuels* **2021**, *35* (11), 9209−9227.

(2) Ahsan, S.; Edgar, M. D.; Krishna, S. H. Understanding Stereochemistry in Biomass Conversion Reactions over Heterogeneous Catalysts. *ACS Sustainable Chem. Eng.* **2024**, *12* (5), 1797−1808.

(3) Overton, J. C.; Engelberth, A. S.; Mosier, N. S. Single-vessel synthesis of 5-hydroxymethylfurfural (HMF) from milled corn. *ACS Sustainable Chem. Eng.* **2020**, *8* (1), 18−21.

(4) Verevkin, S. P.; Emel'yanenko, V. N.; Stepurko, E. N.; Ralys, R. V.; Zaitsau, D. H.; Stark, A. Biomass-Derived Platform Chemicals: Thermodynamic Studies on the Conversion of 5-Hydroxymethylfurfural into Bulk Intermediates. *Ind. Eng. Chem. Res.* **2009**, *48* (22), 10087−10093.

(5) Hu, L.; He, A.; Liu, X.; Xia, J.; Xu, J.; Zhou, S.; Xu, J. Biocatalytic Transformation of 5-Hydroxymethylfurfural into High-Value Derivatives: Recent Advances and Future Aspects. *ACS Sustainable Chem. Eng.* **2018**, *6* (12), 15915−15935.

(6) Zhu, P.; Shi, M.; Shen, Z.; Liao, X.; Chen, Y. Electrocatalytic Conversion of Biomass-Derived Furan Compounds: Mechanisms. *Catalysts and Perspectives. Chemical Science* **2024**, *15*, 4723−4756.

(7) Ji, K.; Xu, M.; Xu, S. M.; Wang, Y.; Ge, R.; Hu, X.; Sun, X.; Duan, H. Electrocatalytic hydrogenation of 5-hydroxymethylfurfural

promoted by a Ru1Cu single-atom alloy catalyst. *Angew. Chem., Int. Ed.* **2022**, *61* (37), No. e202209849.
(8) Wu, Y.; Jiang, Y.; Chen, W.; Yue, X.; Dong, C. L.; Qiu, M.; Nga, T. T. T.; Yang, M.; Xia, Z.; Xie, C.; et al. Selective Electroreduction of 5-Hydroxymethylfurfural to Dimethylfuran in Neutral Electrolytes via Hydrogen Spillover and Adsorption Configuration Adjustment. *Adv. Mater.* **2024**, *36* (7), 2307799.
(9) Guo, L.; Zhang, X.; Gan, L.; Pan, L.; Shi, C.; Huang, Z. F.; Zhang, X.; Zou, J. J. Advances in Selective Electrochemical Oxidation of 5-Hydroxymethylfurfural to Produce High-Value Chemicals. *Advanced Science* **2023**, *10* (4), 2205540.
(10) Zhang, L.; Meng, G.; Zhang, W.; Li, X.; Zhang, Z.; Yang, M.; Wu, Y.; Wang, D.; Li, Y. Oriented Conversion of a LA/HMF Mixture to GVL and FDCA in a Biphasic Solvent over a Ru Single-Atom/Nanoparticle Dual-Site Catalyst. *ACS Catal.* **2023**, *13* (4), 2268−2276.
(11) Li, S.; Wang, S.; Wang, Y.; He, J.; Li, K.; Xu, Y.; Wang, M.; Zhao, S.; Li, X.; Zhong, X.; et al. Doped Mn enhanced NiS electrooxidation performance of HMF into FDCA at industrial-level current density. *Adv. Funct. Mater.* **2023**, *33*, 2214488.
(12) Sanghez de Luna, G.; Ho, P. H.; Lolli, A.; Ospitali, F.; Albonetti, S.; Fornasari, G.; Benito, P. Ag electrodeposited on Cu open-cell foams for the selective electroreduction of 5-hydroxymethylfurfural. *ChemElectroChem.* **2020**, *7* (5), 1238−1247.
(13) Oliver, Z. J.; Abrams, D. J.; Cardinale, L.; Chen, C.-J.; Beutner, G. L.; Caille, S.; Cohen, B.; Deng, L.; Diwan, M.; Frederick, M. O. Scaling Organic Electrosynthesis: The Crucial Interplay between Mechanism and Mass Transport. *ACS Central Science* **2025**, *11*, 528.
(14) Jiang, M.; Tan, J.; Chen, Y.; Zhang, W.; Chen, P.; Tang, Y.; Gao, Q. Promoted electrocatalytic hydrogenation of furfural in a biphasic system. *Chem. Commun.* **2023**, *59* (21), 3103−3106.
(15) Gidi, L.; Amalraj, J.; Tenreiro, C.; Ramírez, G. Recent progress, trends, and new challenges in the electrochemical production of green hydrogen coupled to selective electrooxidation of 5-hydroxymethylfurfural (HMF). *RSC Adv.* **2023**, *13* (40), 28307−28336.
(16) Zhang, Y.; Shen, Y. Electrochemical hydrogenation of levulinic acid, furfural and 5-hydroxymethylfurfural. *Applied Catalysis B: Environmental* **2024**, *343*, 123576.
(17) Hauke, P.; Klingenhof, M.; Wang, X.; de Araújo, J. F.; Strasser, P. Efficient electrolysis of 5-hydroxymethylfurfural to the biopolymer-precursor furandicarboxylic acid in a zero-gap MEA-type electrolyzer. *Cell Reports Physical Science* **2021**, *2* (12), 100650.
(18) Delparish, A.; Uslu, A.; Cao, Y.; de Groot, T.; van der Schaaf, J.; Noel, T.; Fernanda Neira d'Angelo, M. Boosting the valorization of biomass and green electrons to chemical building blocks: A study on the kinetics and mass transfer during the electrochemical conversion of HMF to FDCA in a microreactor. *Chemical Engineering Journal* **2022**, *438*, 135393.
(19) Etminan, A.; Muzychka, Y. S.; Pope, K. A review on the hydrodynamics of Taylor flow in microchannels: Experimental and computational studies. *Processes* **2021**, *9* (5), 870.
(20) Paunovic, V.; Schouten, J. C.; Nijhuis, T. Direct synthesis of hydrogen peroxide in a wall-coated microchannel reactor over Au−Pd catalyst: A performance study. *Catal. Today* **2015**, *248*, 160−168.
(21) Bhuvanendran, N.; Ravichandran, S.; Xu, Q.; Maiyalagan, T.; Su, H. A quick guide to the assessment of key electrochemical performance indicators for the oxygen reduction reaction: A comprehensive review. *Int. J. Hydrogen Energy* **2022**, *47* (11), 7113−7138.
(22) Sanghez de Luna, G.; Ho, P. H.; Sacco, A.; Hernández, S.; Velasco-Vélez, J.-J. s.; Ospitali, F.; Paglianti, A.; Albonetti, S.; Fornasari, G.; Benito, P. AgCu Bimetallic Electrocatalysts for the Reduction of Biomass-Derived Compounds. *ACS Appl. Mater. Interfaces* **2021**, *13* (20), 23675−23688.
(23) Asfia, M. P.; Cuomo, A.; Kloth, R.; Mayrhofer, K. J.; Nikolaienko, P. The Role of Alkali Cations on the Selectivity of 5-Hydroxymethylfurfural Electroreduction on Glassy Carbon. *ChemSusChem* **2024**, *17*, No. e202400535.
(24) Lee, D. K.; Kubota, S. R.; Janes, A. N.; Bender, M. T.; Woo, J.; Schmidt, J.; Choi, K. S. The Impact of 5-Hydroxymethylfurfural (HMF)-Metal Interactions on the Electrochemical Reduction Pathways of HMF on Various Metal Electrodes. *ChemSusChem* **2021**, *14* (20), 4563−4572.
(25) Kloth, R.; Vasilyev, D. V.; Mayrhofer, K. J.; Katsounaros, I. Electroreductive 5-Hydroxymethylfurfural Dimerization on Carbon Electrodes. *ChemSusChem* **2021**, *14* (23), 5245−5253.
(26) Yuan, X.; Lee, K.; Bender, M. T.; Schmidt, J.; Choi, K. S. Mechanistic Differences between Electrochemical Hydrogenation and Hydrogenolysis of 5-Hydroxymethylfurfural and Their pH Dependence. *ChemSusChem* **2022**, *15* (17), No. e202200952.
(27) Li, M.; Zheng, T.; Lu, D.; Dai, S.; Chen, X.; Pan, X.; Dong, D.; Weng, R.; Xu, G.; Wang, F. Facet effect on the reconstructed Cu-catalyzed electrochemical hydrogenation of 5-hydroxymethylfurfural (HMF) towards 2, 5-bis (hydroxymethy) furan (BHMF). *Journal of Energy Chemistry* **2023**, *84*, 101−111.
(28) de Luna, G. S.; Sacco, A.; Hernandez, S.; Ospitali, F.; Albonetti, S.; Fornasari, G.; Benito, P. Insights into the Electrochemical Reduction of 5-Hydroxymethylfurfural at High Current Densities. *ChemSusChem* **2022**, *15*, No. e202102504.
(29) Luo, X.; Xie, C.; Zhao, Z.; Shi, M.; Zheng, H. Optimization of Electrochemical Reduction of Biomass Derived 5-Hydroxymethylfurfural (HMF): A Volcano Plot and Bimetallic Catalysts. *ChemSusChem* **2024**, *17*, No. e202400723.

https://doi.org/10.1021/acssuschemeng.5c04334
ACS Sustainable Chem. Eng. 2025, 13, 12323−12327